Operational Procedures of Agencies Contributing to the ISC

Collm Geophysical Observatory

S. Wendt and P. Buchholz

Institute for Geophysics and Geology, University of Leipzig

Germany

Excerpt from the
Summary of the Bulletin of the International Seismological Centre:

Wendt, S. and Buchholz, P., Collm Geophysical Observatory, *Summ. Bull. Internatl. Seismol. Cent.*, January - June 2014, *51*(I), pp. 32–44, Thatcham, United Kingdom, 2017, doi:10.5281/zenodo.996043.

5

Operational Procedures of Contributing Agencies

5.1 Collm Geophysical Observatory

S. Wendt, P. Buchholz, Institute for Geophysics and Geology, University of Leipzig, Germany

Siegfried Wendt and Petra Buchholz

In this article we will give a short overview of recording and evaluating earthquakes at the Geophysical Observatory in Collm, Germany.

5.1.1 History and Present Status

In the 1920's conditions in Leipzig were more and more disturbed by increasing industrialization and traffic. Ludwig Weickmann, head of the Geophysics Institute since 1923, was looking for a better place for the Wiechert horizontal seismograph, which had been working in Leipzig since 1902, but also for other branches of geophysical research like magnetism, gravity and meteorology. The observatory was built on the slopes of Collm hill near the city of Oschatz and about 50 km east of Leipzig (Fig. 5.1). The main building (Fig. 5.2) was opened in 1932 and the seismometer hut in 1934. Since 1935 station CLL has been working continuously, including during the Second World War. Since 1993 station CLL has been part of the German Regional Seismological Network (GRSN) and is equipped with a STS-2 broadband seismometer with digital data logging and online data transmission. Some generations of analogue seismometers used at CLL, for instance short-period Benioff seismometers, Wood-Anderson torsion instrument, short-period SSJ-2 and long-period SSJ-1 seismometers, developed in Jena, demonstrate technical progress and can be visited. Our Wiechert seismograph with a mass of 1100 kg is still working today (Fig. 5.3). In 2007 the STS-2 seismometer was moved to a new underground vault. Our

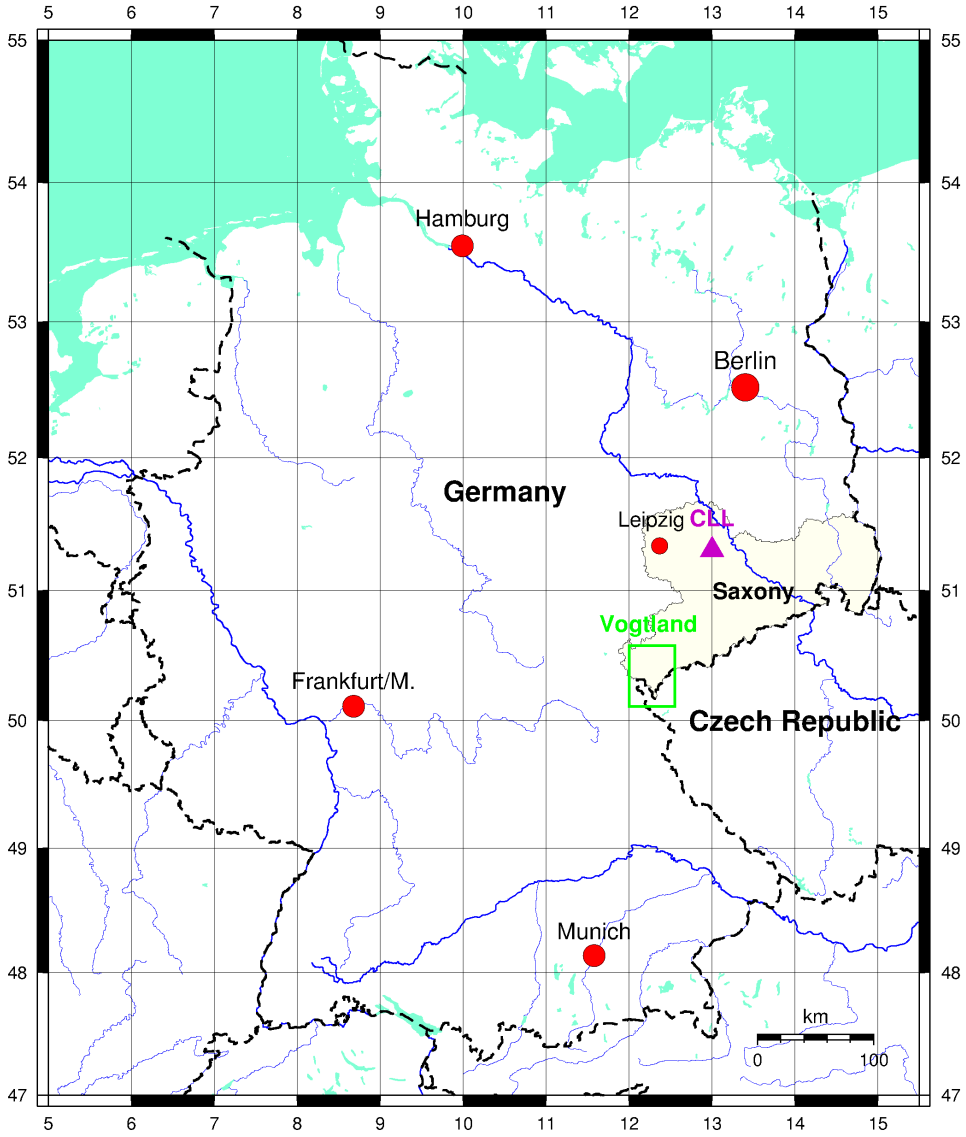

Figure 5.1: *Map of Germany with Saxony, CLL and Vogtland region (see Fig. 5.12).*

analogue archives contain an enormous number of earthquake records, which can be used for processing old events with new methods. Since 1993 wave form data from broadband station CLL is available via the Federal Institute for Geosciences and Natural Resources (BGR) in Hanover:

`http://www.bgr.bund.de/DE/Themen/Erdbeben-Gefaehrdungsanalysen/Seismologie/Seismologie/Datenzentrum/waveform_request/waveform_request_node.html`.

The observatory also accommodates equipment for other geophysical research. Ludwig Weickmann was a meteorologist interested in microclimatic investigations. In 1956 Rudolf Schminder began with LF measurements, which use low-frequency radio waves, of the wind in the ionosphere. Magnetic measurements (variation of magnetic field of the earth) completed ionospheric investigations. A VHF (very high frequency) meteor radar was installed at Collm in 2004 to replace the LF measurements. Both methods were used until LF measurements were stopped in 2007.

The geographical co-ordinates of station Collm (CLL) are: Latitude 51.3077°N, Longitude: 13.0026°E, Elevation: 230 m.

Figure 5.2: *Main building of Collm Geophysical Observatory (Petra Buchholz, 2017).*

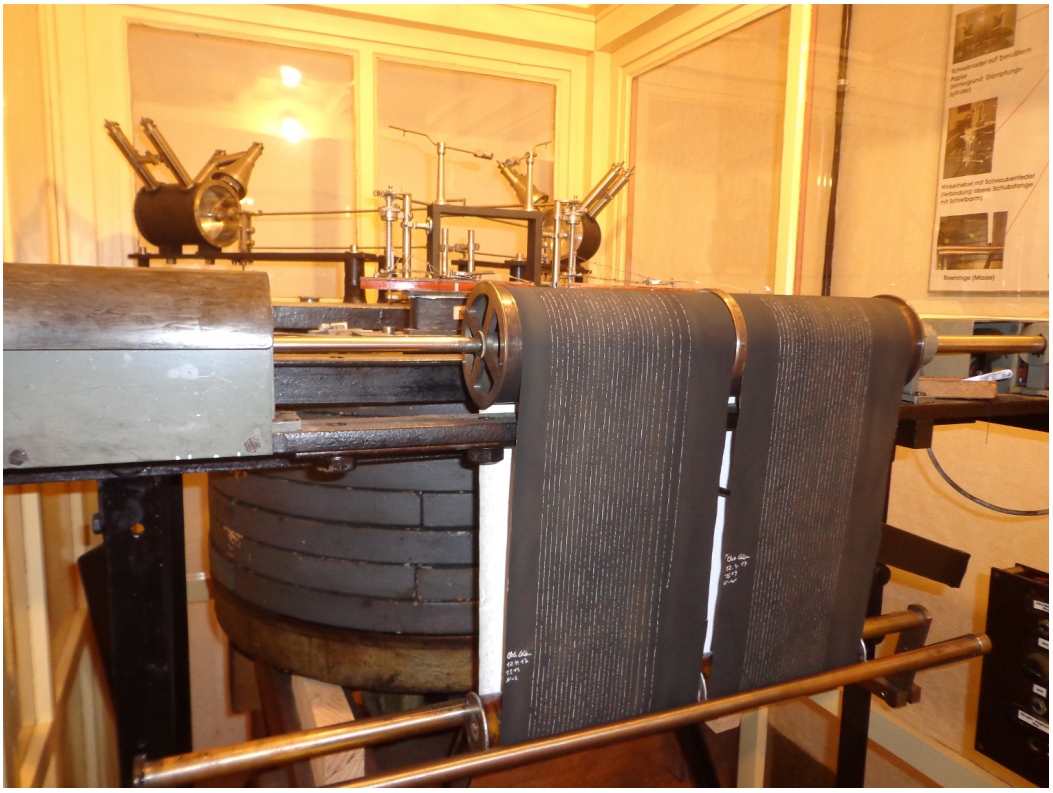

Figure 5.3: *Wiechert seismograph still working in seismometer hut (Petra Buchholz, 2017).*

Year	Number of events	Events with source parameters
2006	5329	4113
2007	5398	4341
2008	5802	4694
2009	4992	3434
2010	4981	3996
2011	8026	6372
2012	5611	4826
2013	5658	4614
2014	6720	5501
2015	5214	4395
Sum	**57731**	**46286**

Table 5.1: *Number of earthquakes evaluated in CLL per year.*

5.1.2 Data Analysis

In general we use CLL broadband data for seismogram interpretation which includes manual phase picking, identification of phases, and magnitude estimation. The data is analysed with Seismic Handler (*Stammler*, 1993). We use GRSN stations to help interpret complicated seismograms with superposition of two events where estimating the slowness is helpful. We calculate many magnitudes and study the various relations between them: beside mb, mB, Ms_20 and Ms_BB also magnitudes for P, PP (short- and long-periodic, on vertical and horizontal components), S and surface waves (also for periods outside the 18 to 22 s window). For local events we estimate Ml and MSgV.

Twice per week we send the results of our seismogram readings to the data centre GSR in Moscow and to our neighbouring stations. One year behind real-time we send our interpretation in a final version to the ISC. This data is completed by source parameters from NEIC or CSEM yielding to our bulletin, which is the basis for some of the figures in this article.

CLL station recorded about 4500 earthquakes per year on average over the last 10 years. Table 5.1 contains numbers of events per year and Figure 5.4 shows a histogram of events per month subdivided into magnitude classes. The maximum amount of recorded events was reached in March 2011 when the Tohoku earthquake with its large aftershocks sequence occurred. In 2008, 2011, and 2014 we recorded a lot of events in NW Czech Republic, less than 10km away from the German-Czech border.

Figure 5.5 represents the global seismicity with more than 46000 earthquakes recorded by CLL during ten years. Blue isolines represent the travel times of the primary longitudinal waves in 2-minute steps. Magnitude mb over epicentral distance and histograms of events over epicentral distance are shown in Figure 5.6. Most of the recorded events are teleseismic events with two peaks between 75° to 85° (the very active regions Japan, Kurile, and Kamchatka) and 145° to 155° (SW Pacific region with Fiji, Tonga, and Kermadec Islands). Recording conditions mainly depend on epicentral distance but also on focal depth. The large number of local events is caused by seismic activity in the German-Czech border region. About 80 percent are swarms and series of quakes in the NW part of Czech Republic.

Figure 5.7 shows histograms of magnitudes mb and MSZ (=Ms_20) and the correlation mb-MSZ for

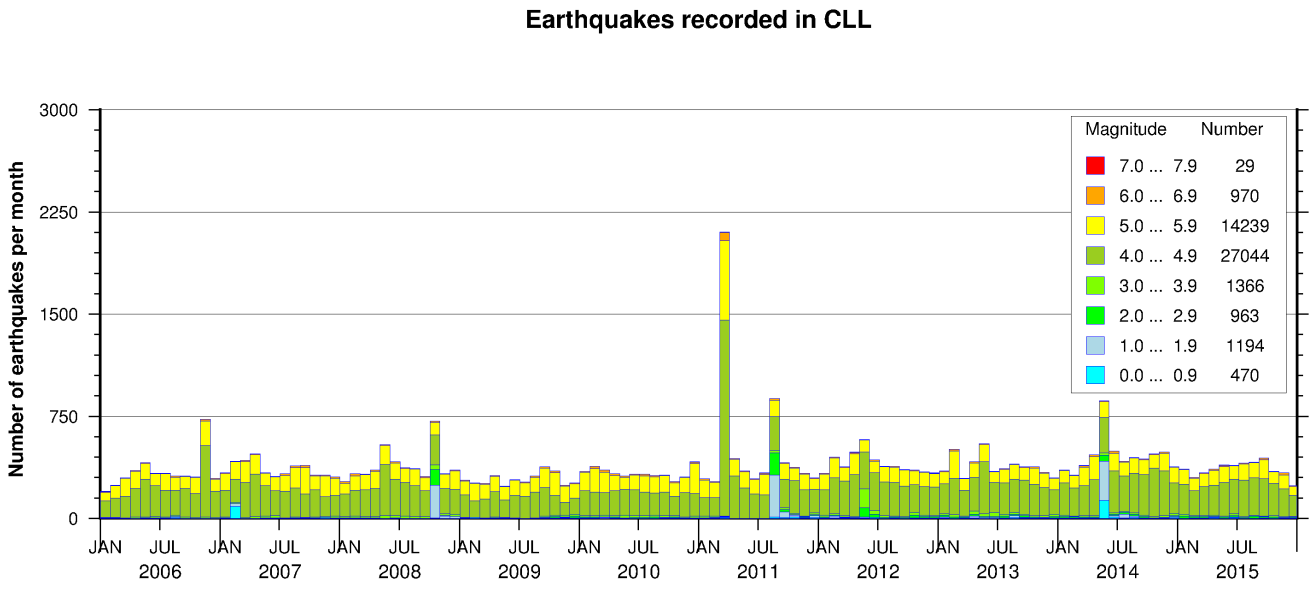

Figure 5.4: *Histogram with earthquakes per month evaluated at CLL.*

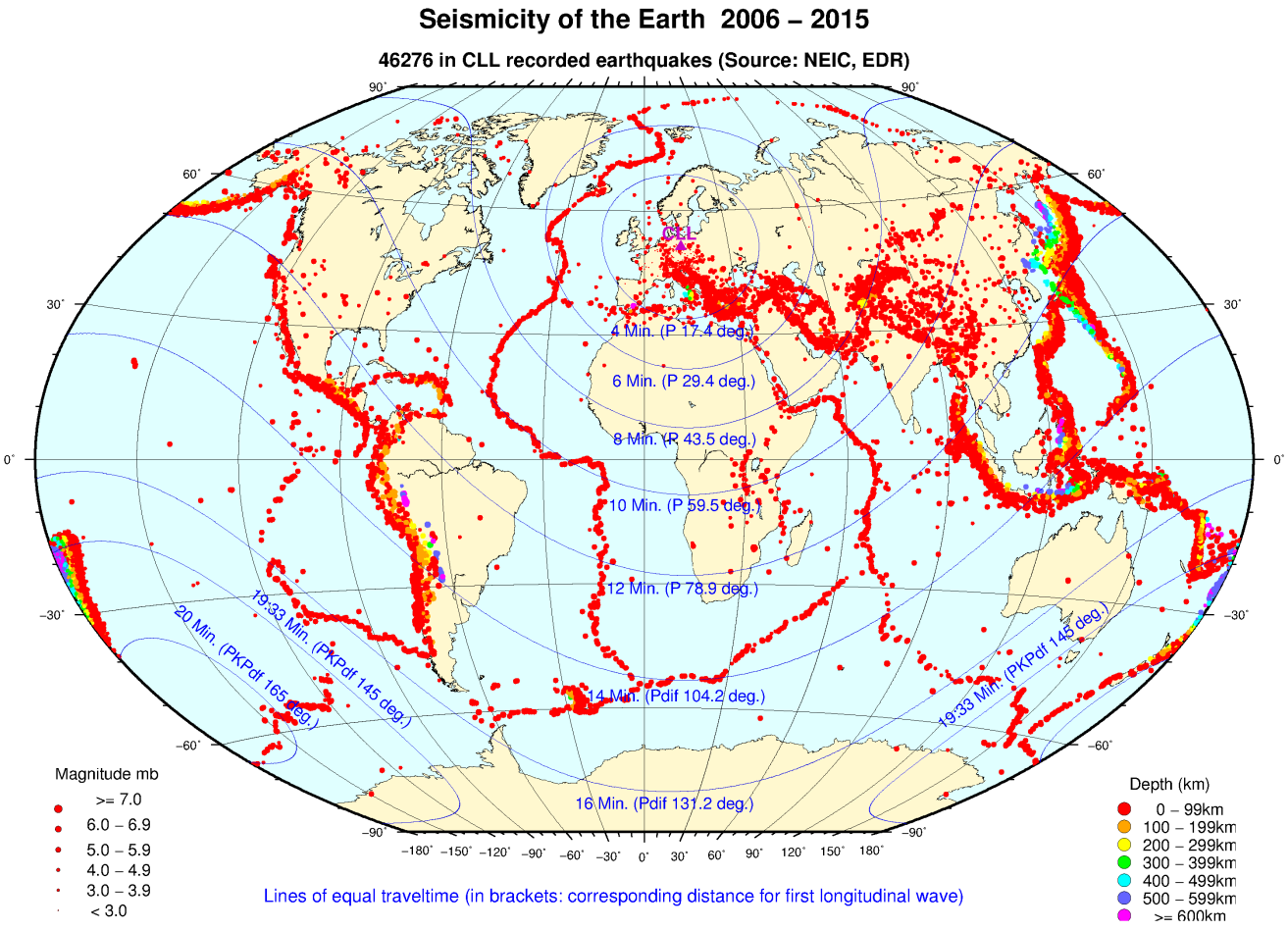

Figure 5.5: *Map of global seismicity with more than 46000 epicenters of earthquakes recorded at CLL. (Earthquake data retrieved from NEIC, ftp://hazards.cr.usgs.gov/NEICPDE/isf2.0/)*

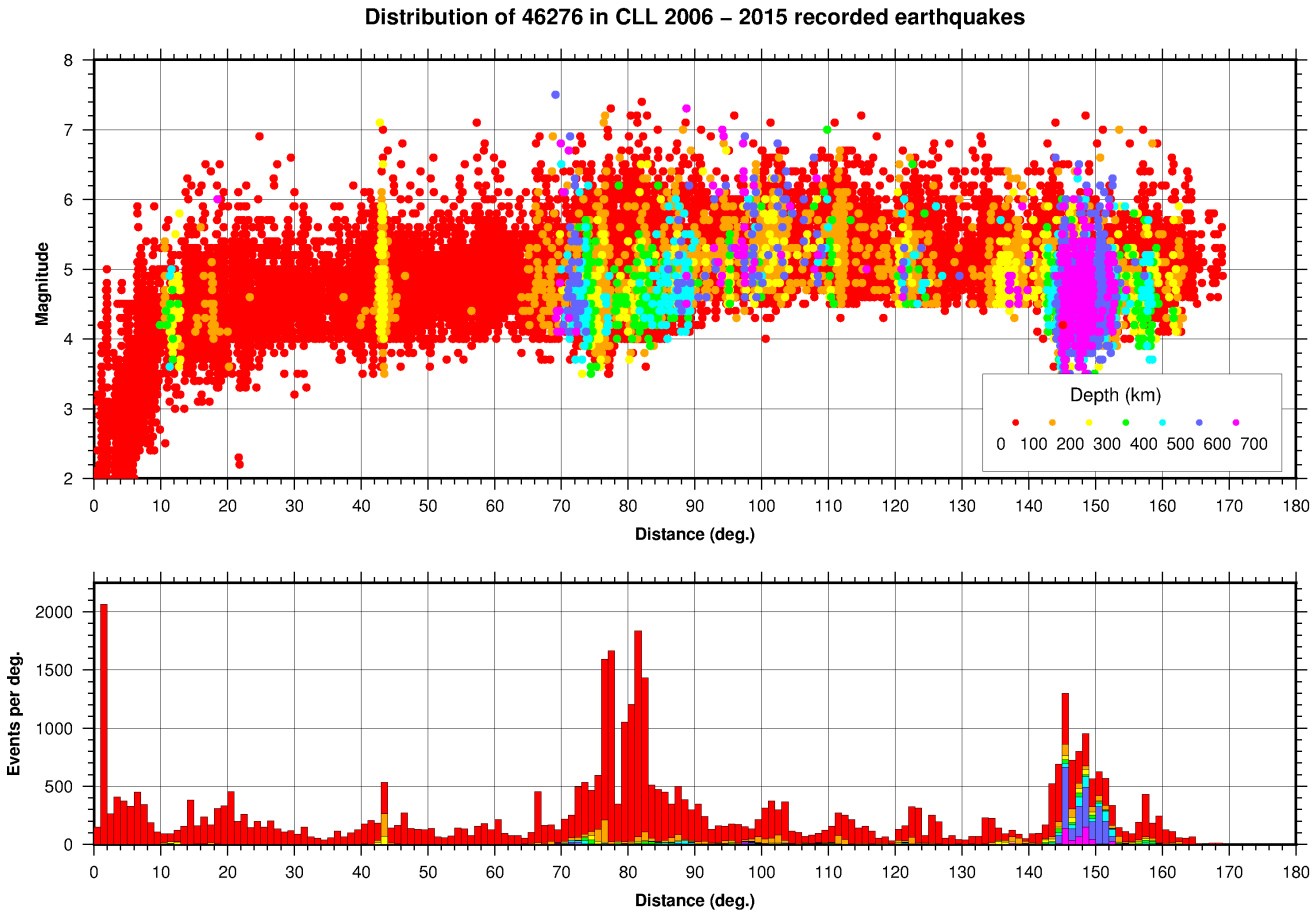

Figure 5.6: *Top: Distribution of mb (Ml for local events) versus epicentral distance colour coded by depth. Bottom: Histogram of events with magnitude mb over epicentral distance colour coded by depth.*

recorded events at CLL. For large quakes with mb $\geq$ 6.0, around where mb saturates, the surface wave magnitude MSZ is greater than body wave magnitude mb. For small quakes mb dominates. In Figure 5.8 we compare three source regions with quite different recording conditions: (1) Kurile Islands (centre) with very good recording conditions at CLL. The first onsets are pure mantle P-waves from an average distance of 77°. (2) Our station has very bad recording conditions for earthquakes in Chile and the Sunda Arc (left) because they nucleate close to the P-wave shadow zone. Pdiff in a distance of about 110° can only be observed for strong earthquakes. The first detectable phase in a seismogram often is PP and in many cases we recorded only surface waves. (3) We have very good recording conditions for PKP waves from source regions in Fiji, Tonga, and Kermadec (right). The histogram of Fiji shows that we record nearly all events with magnitudes larger than mb=5.0. The good propagation conditions for PKP waves can result in the recording of late and very late core phases (P'N,PNKP). Figure 5.9 shows travel times of such phases and Figure 5.10 the corresponding ray paths in the Earth. Misinterpretation of late and very late core phases as P phases can yield to the creation of bogus earthquakes. We appreciate the interpretation of complicated seismograms with many phases (Fig. 5.11).

5.1.3 Local Network

In 2000 the installation of a local network (SXNET) in Vogtland region began (network administrator: Sigward Funke, University of Leipzig). A map of station distribution and epicenters for the years 2009

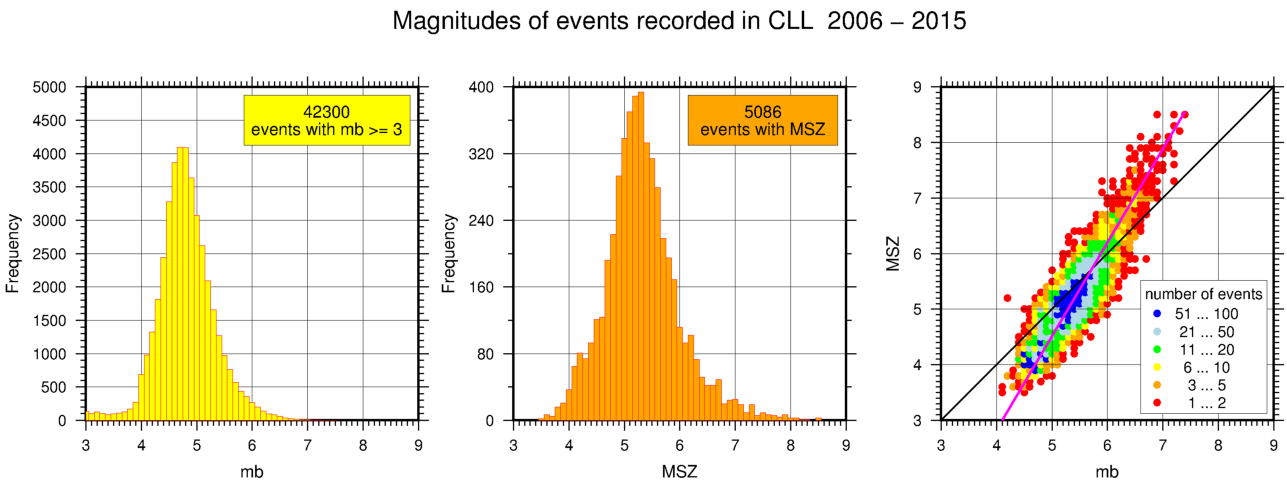

Figure 5.7: *Histograms of distribution of mb and MSZ and correlation mb-MSZ.*

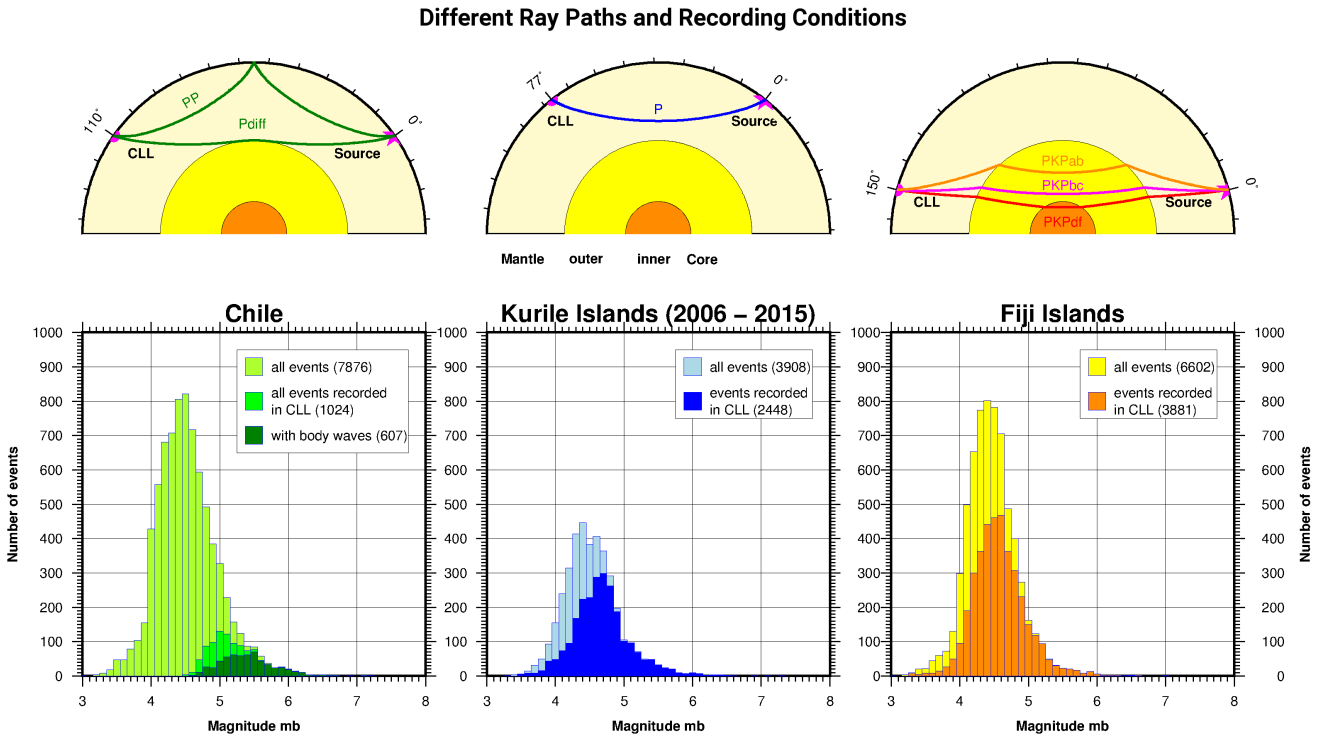

Figure 5.8: *Different recording conditions for three source regions: Chile, Kuril Islands, and Fiji Islands and the corresponding ray paths in the Earth. Light coloured histograms in the back are magnitude distributions of all events given by NEIC in Earthquake Data Report (EDR), whereas dark coloured histograms in the front are events recorded at CLL.*

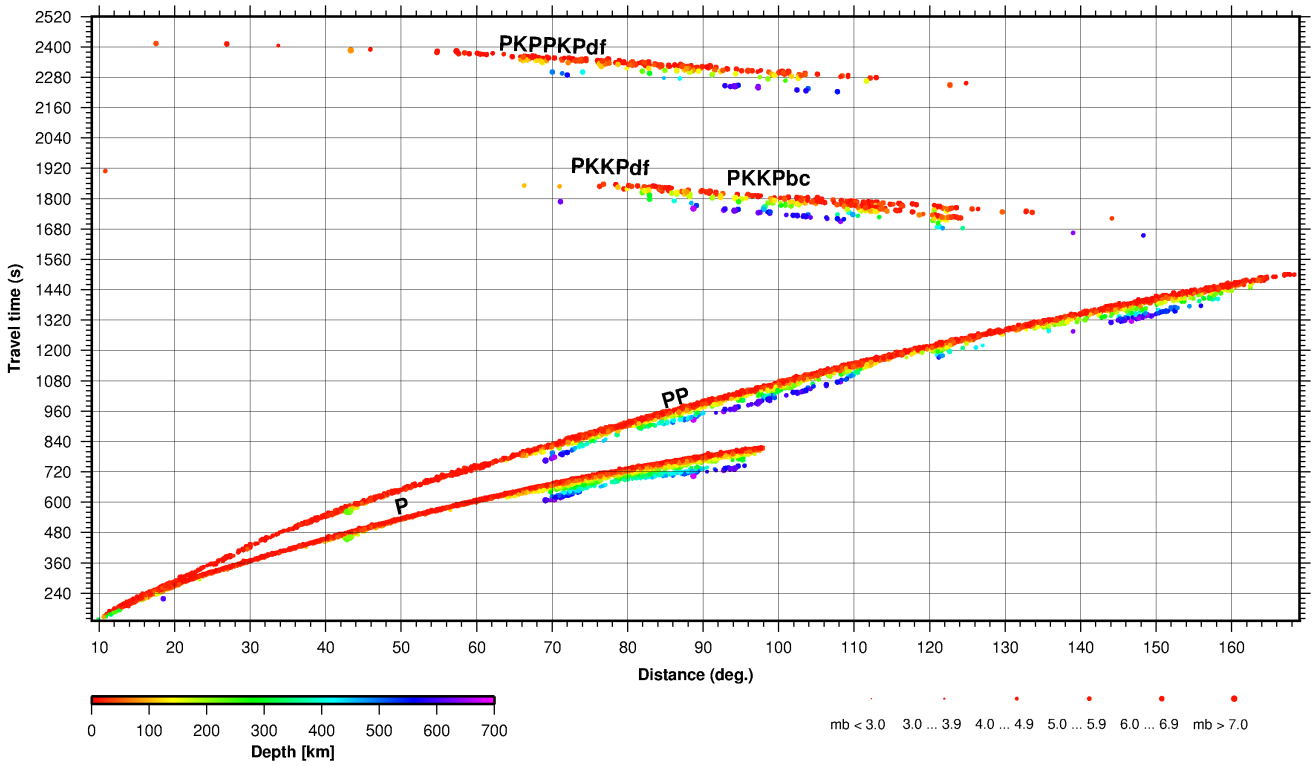

Figure 5.9: *Travel times of P, PP, PKKPdf, PKKPbc, and PKPPKPdf colour coded by depth.*

to 2016 is shown in Figure 5.12 while Figure 5.13 shows the time distribution of local magnitudes.

At Collm Observatory we detect and manually pick regional events recorded by the network on a daily basis. The picks and hypocenters of local events larger than Ml 2.0 are also included in our reports to the ISC. We use Seisan (*Havskov and Ottemöller*, 1999) for manual phase picking and amplitude measurements. 100-Hz waveform data for more than 30 stations is available from several networks, generally: SXNET (network, Saxony), TSN (network, Thuringia), NKC (Station, Czech Republic), VIEL (Station, Bavaria). The distance between stations in Upper Vogtland region is 10 to 15 km. We evaluate on an average 1200 local earthquakes per year of which about 80 percent are events located in the NW part of the Czech Republic less than 10 km away from the German-Czech border. Our data base contains more than 13000 local events with magnitudes ranging from -1.2 to 4.2. Even standard seismogram evaluation yields to good results with respect to the quality of epicenter location and depth. Location and magnitude estimates can be substantially improved by applying station corrections. To account for variations in seismic velocity we use different velocity models for different geographical epicentral regions. When only a small amount of data is available we search for the best velocity model with the lowest RMS by stepwise changing the velocity and depth of a layer. Events large enough for macroseismic observation are reliably detected and located by automatic systems as SeisComP3 (`http://www.seiscomp3.org`) and RTQUAKE (*Utheim et al.*, 2014).

To characterize the quality of a hypocentre location we follow the criteria given in the Seisan manual (*Havskov and Ottemöller*, 1999). Distributive criteria (Fig. 5.14) describe the network configuration as number of stations used, distance to nearest station, or azimuthal gap, whereas statistical criteria (Fig. 5.15) show location errors mainly caused by the quality of picked arrival times and the applied velocity model. Table 5.2 shows the codes for the different quality classes used in Figures 5.14 and 5.15.

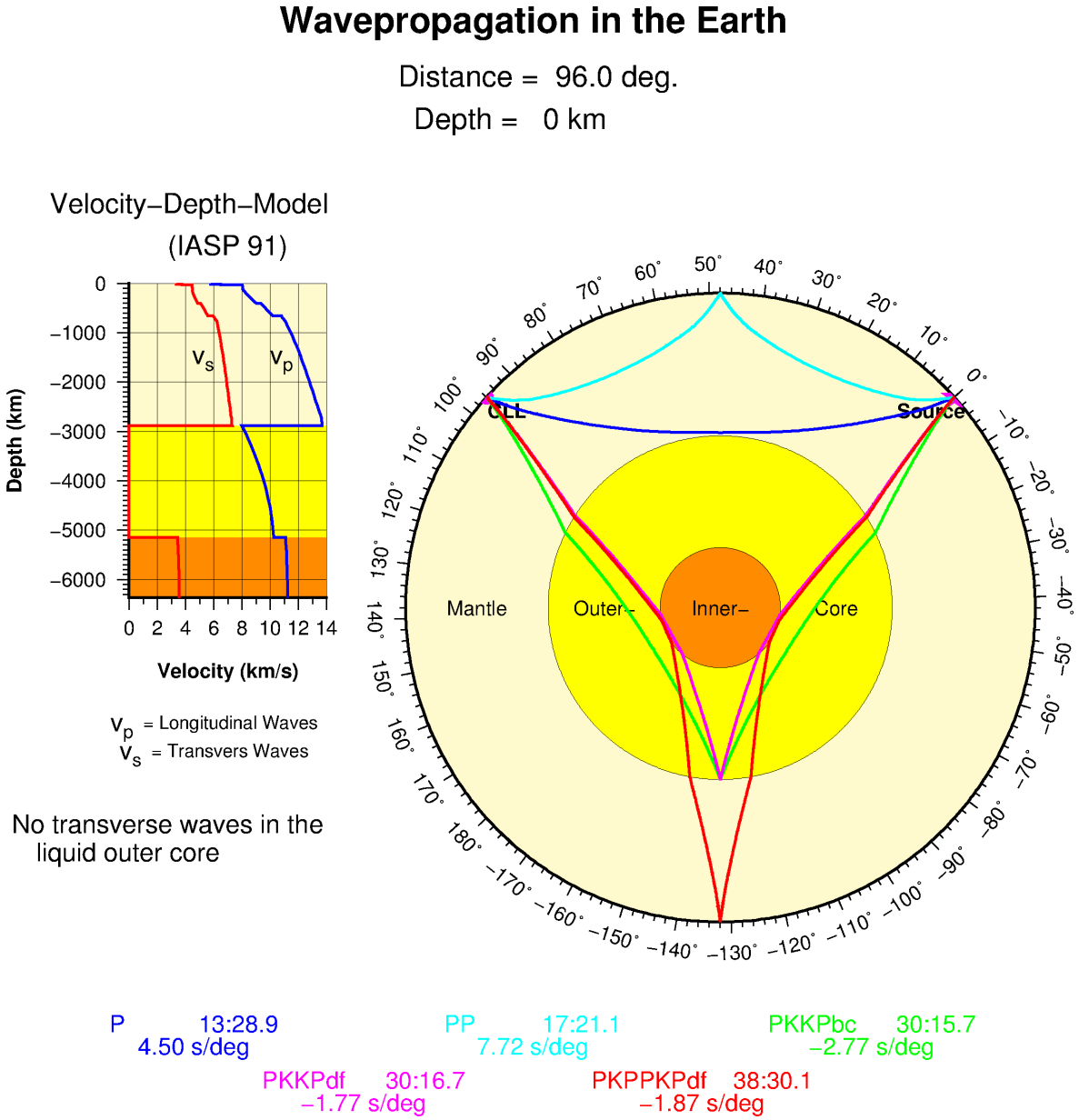

Figure 5.10: *Ray paths in the inner Earth for P, PP, PKKPdf, PKKPbc, and PKPPKPdf. On the right side of the phase names are travel times, below slowness.*

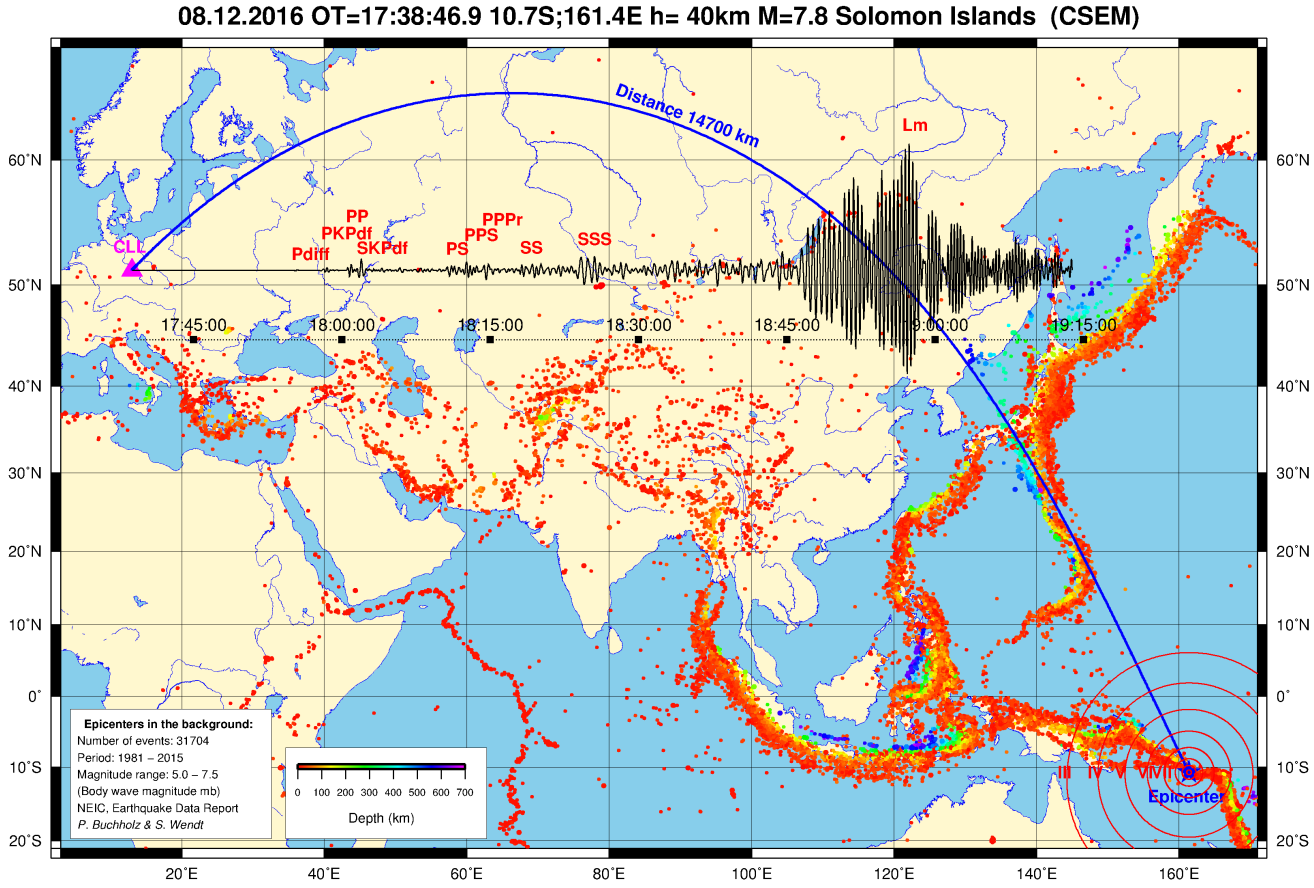

Figure 5.11: *Map with background seismicity and example of a seismogram with many phases from a 7.8 event in the Solomon islands recorded by CLL.*

Quality	Distributive	Statistical
Excellent	a / Circle	A / Red
Good	b / Pentagon	B / Yellow
Fair	c / Diamond	C / Green
Poor	d / Triangle	D / Blue

Table 5.2: *Codes for different quality classes (Fig. 5.14 and 5.15).*

In some histograms the horizontal axis is colour coded by quality, e.g. a azimuthal gap between 0° and 90° is considered "excellent" and marked in red in the upper left image of Figure 5.14. The longitudinal location errors show higher values than the latitudinal errors (Fig. 5.15, top left and middle) which is due to the network being elongated predominantly in NS direction. The RMS errors (Fig. 5.15, bottom left) almost all fall in the highest quality class confirming the high quality of the velocity models. The combination of all single qualities give the total quality of a location. The matrix in Figure 5.15 (bottom middle) shows the number of events by quality classes Aa to Dd, e.g. 58 events are of the highest quality Aa which is reflected by a red circle. Depicting the quality classes with coloured shapes makes it easy to identify the quality of an event location in maps.

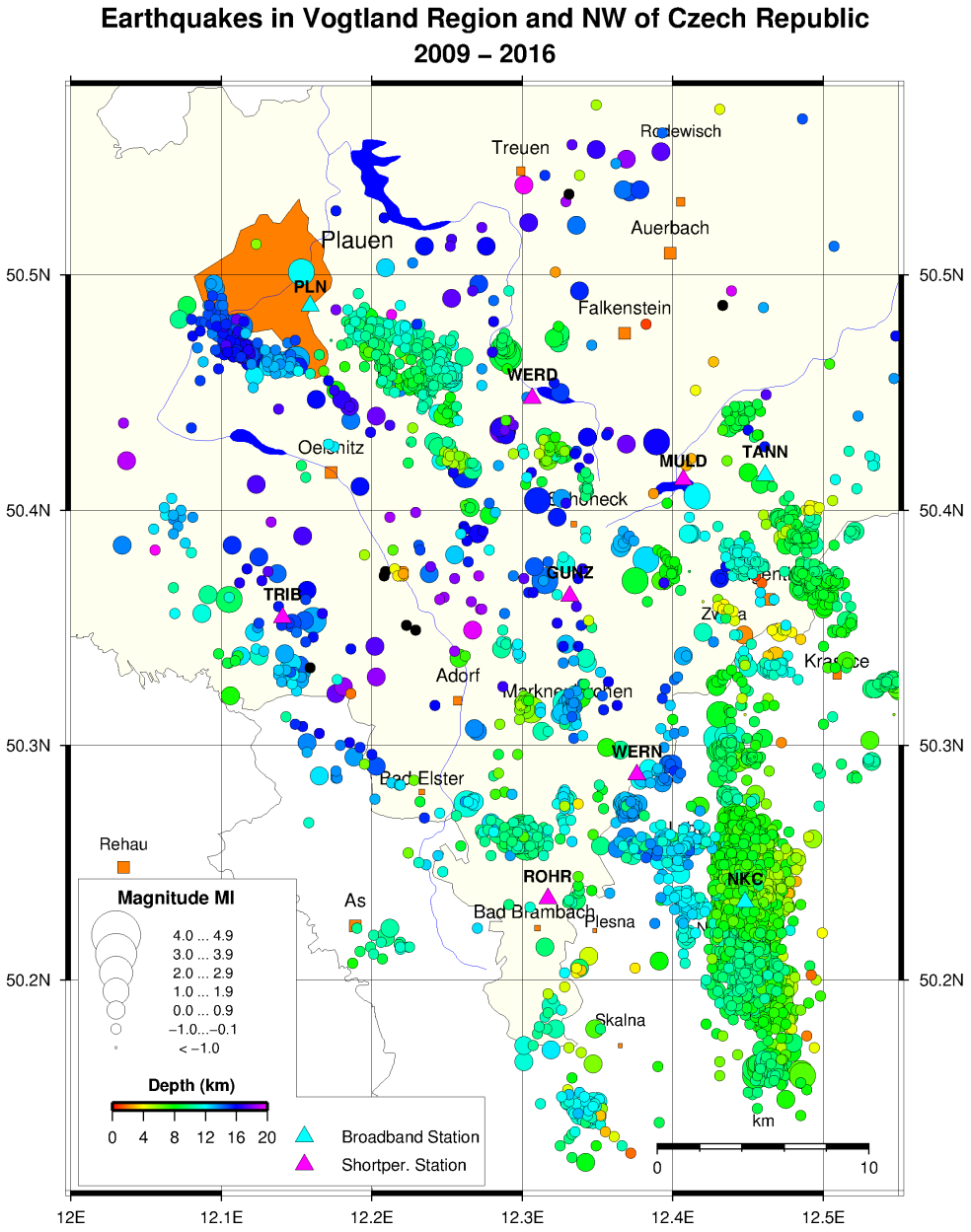

Figure 5.12: *Epicenters of Vogtland region and NW part of Czech Republic (see green box in Fig. 5.1).*

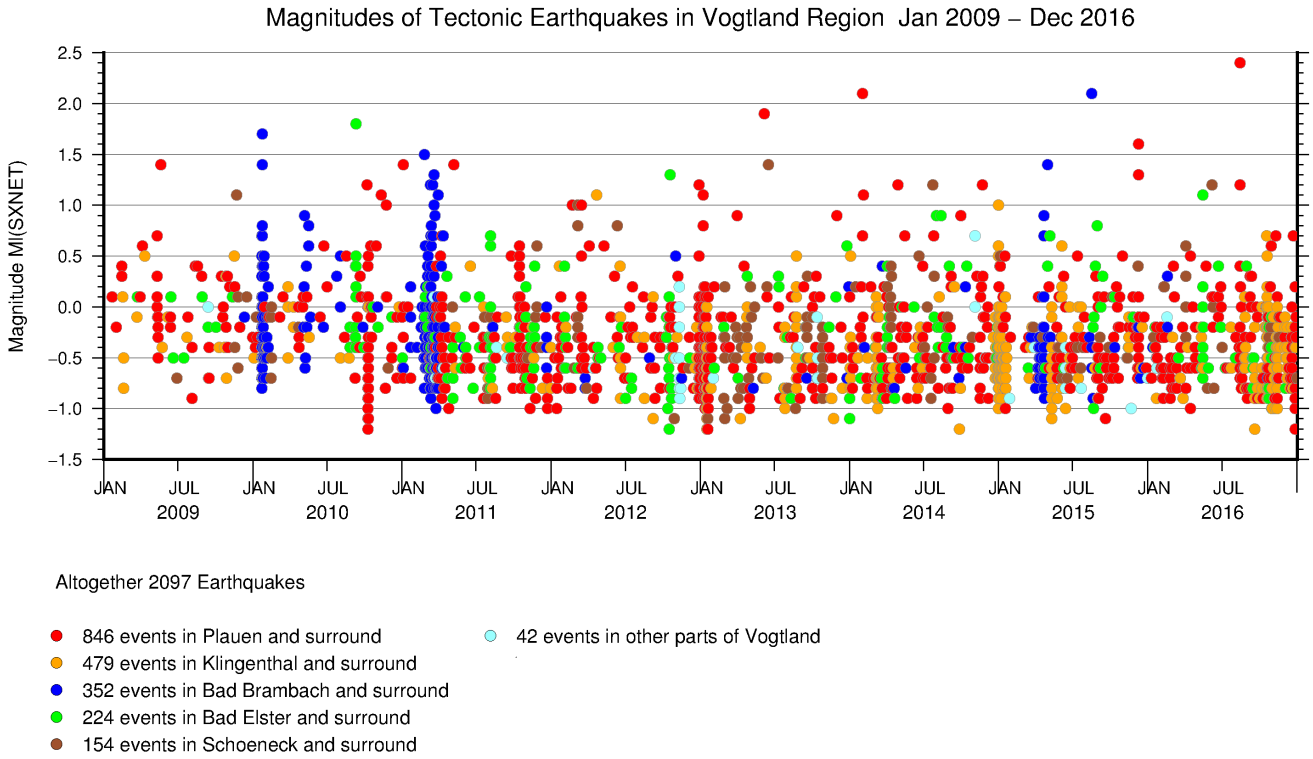

Figure 5.13: *Local Magnitude Ml versus time (only for Vogtland region).*

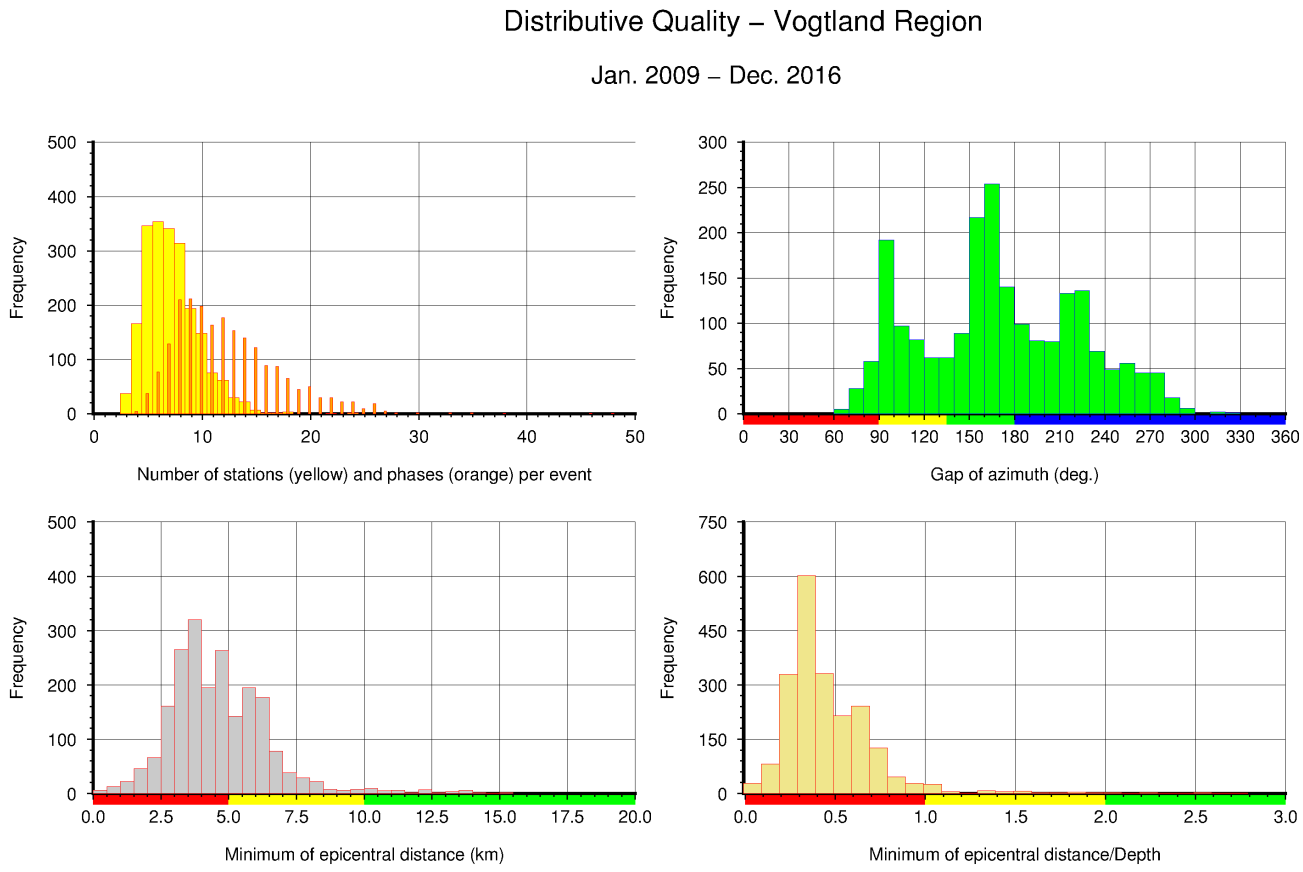

Figure 5.14: *Distributive quality for Vogtland region. Colours on horizontal axis represent quality class, where red=excellent, yellow=good, green=fair, and blue=poor. See text for more information.*

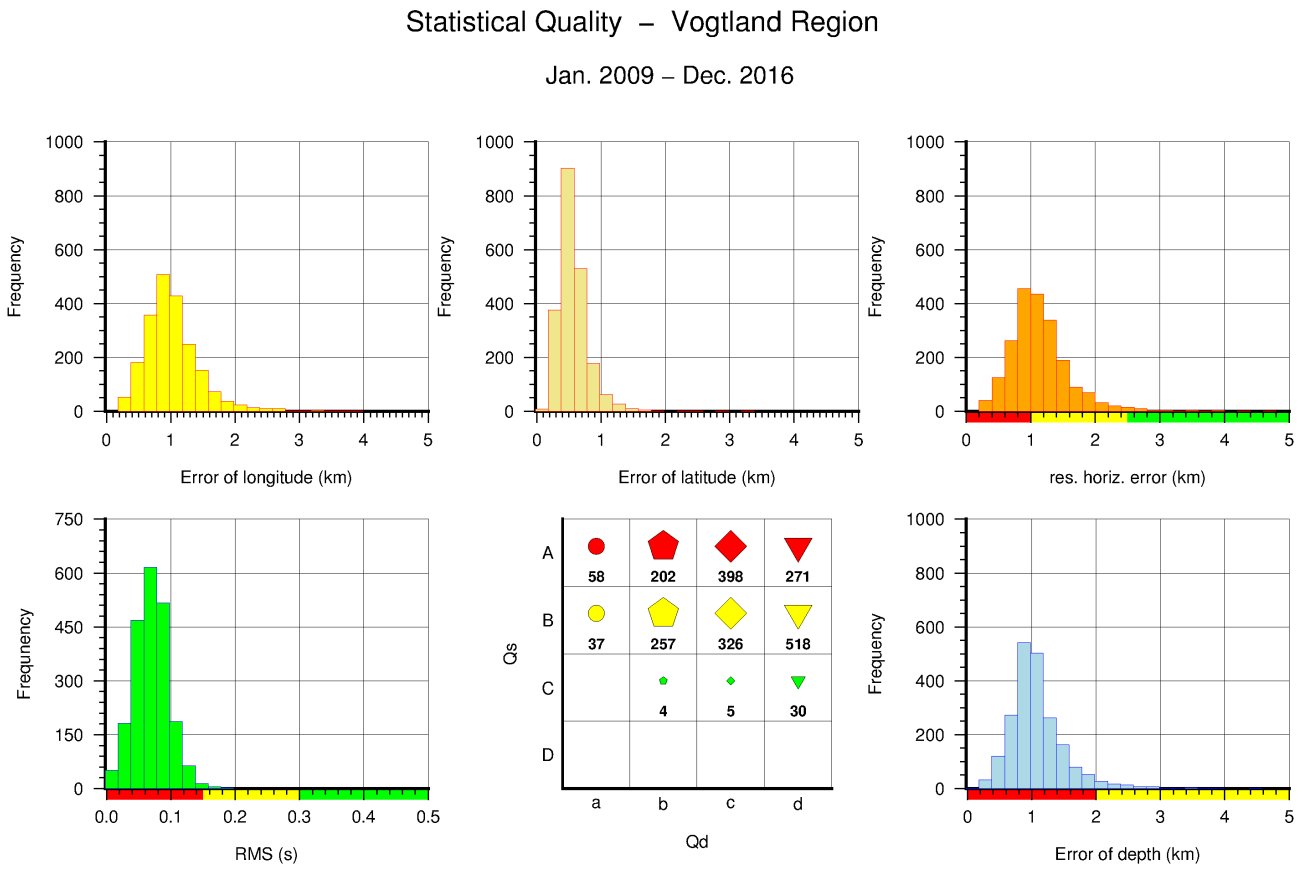

Figure 5.15: *Statistical quality for Vogtland region. Bottom middle: Matrix showing distribution of location qualities. Colours represent quality class, where red=excellent, yellow=good, green=fair, and blue=poor. See text for more information.*

5.1.4 Acknowledgements

The authors are grateful to editor Kathrin Lieser for her enormous help in designing this manuscript and for her very helpful suggestions. We thank the developers of Generic Mapping Tool (GMT) Paul Wessel and Walter H.F. Smith for powerful software which we have used for producing some of the figures.

5.1.5 References

Havskov, J. and L. Ottemöller (1999), SeisAn Earthquake analysis software, *Seismological Research Letters*, *70*(5), 532–534.

Stammler, K. (1993), Seismic Handler – Programmable multichannel data handler for interactive and automatic processing of seismological analyses, *Computers & Geosciences*, *19*(2), 135–140, `http://www.seismic-handler.org`, DOI:10.1016/0098-3004(93)90110-Q.

Utheim, T., J. Havskov, M. Ozyazicioglu, J. Rodriguez, E. Talavera (2014), RTQUAKE, A Real-Time Earthquake Detection System Integrated with SEISAN, *Seismological Research Letters*, *85*(3), 735–742, DOI:10.1785/0220130175.